Lipids and Lipoproteins:

Separation and Identification of Major Plant Sphingolipid Classes from Leaves

Jonathan E. Markham, Jia Li, Edgar B. Cahoon and Jan G. Jaworski

J. Biol. Chem. 2006, 281:22684-22694.
doi: 10.1074/jbc.M604050200 originally published online June 12, 2006

THE JOURNAL OF BIOLOGICAL CHEMISTRY VOL. 281, NO. 32, pp. 22684–22694, August 11, 2006
Printed in the U.S.A.

Separation and Identification of Major Plant Sphingolipid Classes from Leaves*

Received for publication, April 27, 2006, and in revised form, June 9, 2006 Published, JBC Papers in Press, June 12, 2006, DOI 10.1074/jbc.M604050200

Jonathan E. Markham[‡1], **Jia Li, Edgar B. Cahoon**[§], **and Jan G. Jaworski**[‡]

From the [‡]*Donald Danforth Plant Science Center and* [§]*United States Department of Agriculture-Agricultural Research Service Plant Genetics Research Unit, Saint Louis, Missouri 63132*

Sphingolipids are major components of the plasma membrane, tonoplast, and other endomembranes of plant cells. Previous compositional analyses have focused only on individual sphingolipid classes because of the widely differing polarities of plant sphingolipids. Consequently, the total content of sphingolipid classes in plants has yet to be quantified. In addition, the major polar sphingolipid class in the model plant *Arabidopsis thaliana* has not been previously determined. In this report, we describe the separation and quantification of sphingolipid classes from *A. thaliana* leaves using hydrolysis of sphingolipids and high performance liquid chromatography (HPLC) analysis of *o*-phthaldialdehyde derivatives of the released long-chain bases to monitor the separation steps. An extraction solvent that contained substantial proportions of water was used to solubilized >95% of the sphingolipids from leaves. Neutral and charged sphingolipids were then partitioned by anion exchange solid phase extraction. HPLC analysis of the charged lipid fraction from *A. thaliana* revealed only one major anionic sphingolipid class, which was identified by mass spectrometry as hexose-hexuronic-inositolphosphoceramide. The neutral sphingolipids were predominantly composed of monohexosylceramide with lesser amounts of ceramides. Extraction and separation of sphingolipids from soybean and tomato showed that, like *A. thaliana*, the neutral sphingolipids consisted of ceramide and monohexosylceramides; however, the major polar sphingolipid was found to be *N*-acetyl-hexosamine-hexuronic-inositolphosphoceramide. In extracts from *A. thaliana* leaves, hexose-hexuronic-inositolphosphoceramides, monohexosylceramides, and ceramides accounted for ~64, 34, and 2% of the total sphingolipids, respectively, suggesting an important role for the anionic sphingolipids in plant membranes.

Sphingolipids are recognized as universal components of eukaryotic membranes with a diverse array of functions (1–3). Recent interest in sphingolipids from plants has been stimulated by the realization that they may form a significant proportion of the plasma membrane (4), potentially as lipid rafts (5, 6), are involved in signaling a plant's response to drought (7, 8), and regulate the ultimate fate of plant cells through programmed cell death (9, 10). In order to understand the role of plant sphingolipids in this diverse array of already discovered roles and to determine what other biological functions sphingolipids may have in plants, it is necessary to be able to measure the sphingolipid content in a qualitative and quantitative way (11). Sphingolipid signaling is thought to be a complex multifactorial signal derived from the interaction of several different sphingolipids (12), making the examination of all sphingolipids a critical factor in the dissection of sphingolipid function. Thus, the emerging field of sphingolipidomics has received much attention in animal biology but remains neglected in plants (13).

Previous studies on plant sphingolipids have exclusively concentrated on single sphingolipid classes (14–17). Neutral sphingolipids, such as ceramide and monohexosylceramide, are easily purified from plants. Since they are soluble in chloroform and resistant to mild-base hydrolysis, they can be purified to near homogeneity with relative ease (18). This has made them a prime target for study by a variety of methods from a wide array of species (18, 19). Glycosylinositolphosphoceramides (GIPCs)[2] are not so amenable to purification, however, and little research has been carried out on their prevalence or occurrence in plants since their initial characterization some 30–40 years ago (20, 21). GIPCs (also referred to as phytoglycolipid) isolated from corn, soybean, and tobacco were found to have the general structure (*N*-acetyl)glucosamine-glucuronic-inositolphosphoceramide with the addition of additional hexoses and pentoses at either the inositol or glucosamine residues (22, 23).

The proportion of total sphingolipids that the GIPCs represent is currently not known. Release of long-chain bases (LCBs) from sphingolipids by hydrolysis of an entire tissue sample is substantially different from that released by hydrolysis of monohexosylceramides purified from the same source (24). The implication is that the nonmonohexosylceramide component of plant sphingolipids is a substantial portion of the total sphingolipid pool.

The problems addressed in this study are as follows. 1) What is the total sphingolipid content of *Arabidopsis thaliana*; 2) what is the relative contribution of individual sphingolipid species to the total sphingolipid content; and 3) what is the nature of the different sphingolipid species? Answering these questions required the development of protocols for the complete

* This work was supported by National Science Foundation 2010 Grant 0312559. The costs of publication of this article were defrayed in part by the payment of page charges. This article must therefore be hereby marked "*advertisement*" in accordance with 18 U.S.C. Section 1734 solely to indicate this fact.

[1] To whom correspondence should be addressed: Donald Danforth Plant Science Center, 975 N. Warson Rd., Saint Louis, MO 63132. Tel.: 314-587-1644; Fax: 314-587-1744; E-mail: jmarkham@danforthcenter.org.

[2] The abbreviations used are: GIPC, glycosylinositolphosphoceramide; HPLC, high performance liquid chromatography; fw, fresh weight; LCB, long-chain base; IPC, inositolphosphoceramide; MS^3, hybrid tandem mass spectrometry with linear ion trap fragmentation.

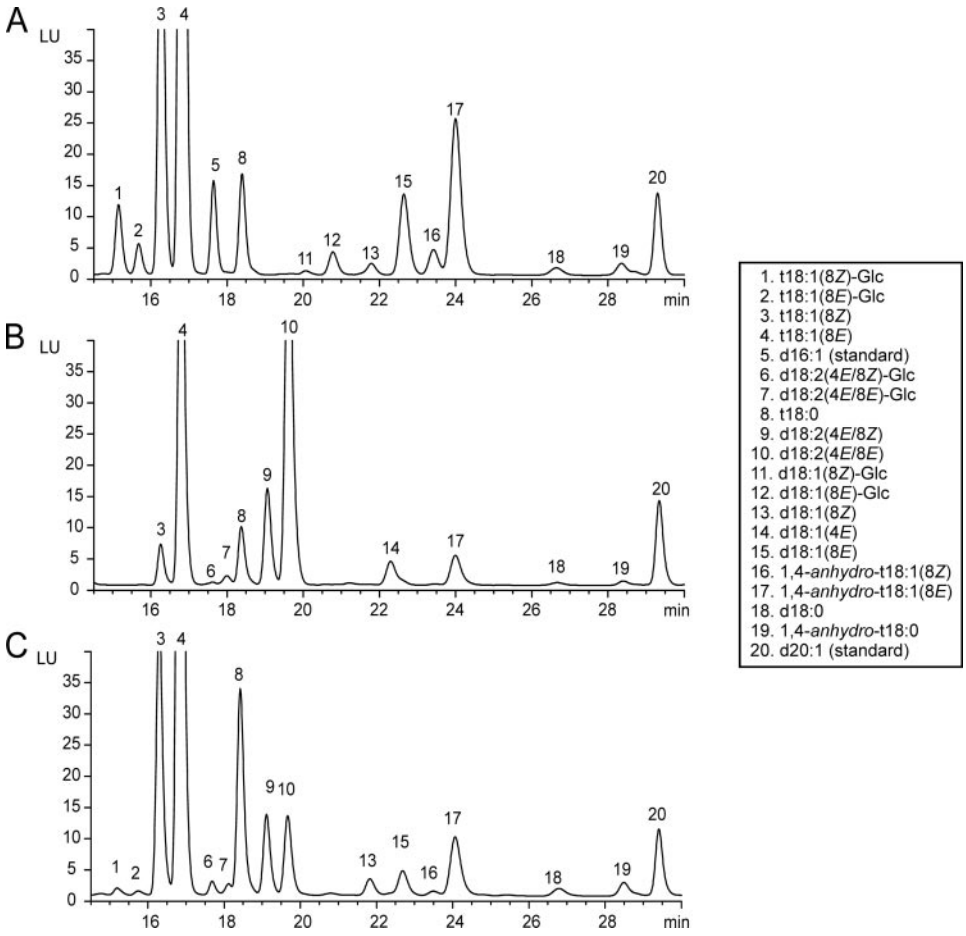

FIGURE 1. **HPLC of *o*-phthaldialdehyde derivatives of plants LCBs.** LCBs were liberated by hydrolysis from leaf tissue of *Arabidopsis* (*A*), tomato (*B*), and soybean (*C*), converted to their *o*-phthaldialdehyde derivatives, and separated by HPLC, as described under "Experimental Procedures." No LCBs eluted in the first 15 min of the run. Peak nomenclature in the *key* is systematic based upon the 2-amino-acyl backbone of the LCB. Hence, t18:0 represents 2-aminooctadecane-1,2,4-triol, trivial name phytosphingosine; t18:1(8*Z*) represents (*Z*)-2-aminooctadec-8-ene-1,2,4-triol, trivial name, (8*Z*)-phytosphingenine; d18:1(4*E*) represents (*E*)-2-aminooctadec-4-ene-1,2-diol, trivial name sphingosine; d18:2(4*E*/8*Z*) represents (*E*,*Z*)-2-aminooctadeca-4,8-dienine-1,2-diol, trivial name (4*E*,8*Z*)-sphingadienine; d18:0 represents 2-aminooctadecane-1,2-diol trivial name sphinganine; d18:1(8*Z*)-Glc represents (*Z*)-glucosyl-1–1′-2-aminooctadec-8-ene-1,2-diol; 1,4-anhydro-t18:1(8*Z*) represents (*Z*)-4-amino-2-(tetradec-4-enyl)-tetrahydrofuran-3-ol; d16:1 represents (*E*)-2-aminohexadec-4-ene-1,2-diol; and d20:1 represents (*E*)-2-aminoeicosan-4-ene-1,2-diol. The d16:1 internal standard, *peak 5*, was used with *Arabidopsis* (*A*) but was not suitable for use in tomato (*B*) or soybean (*C*) due to the presence of overlapping *peaks 6* and *7*.

extraction of all sphingolipids from plants and their separation by chromatography. To demonstrate general applicability of the protocols used to answer these problems and to serve as a comparison, a similar analysis of the sphingolipid content of tomato and soybean was also performed. In all cases, the GIPCs were shown to represent a substantial proportion of the total sphingolipid.

EXPERIMENTAL PROCEDURES

Materials

Except where noted, all chemicals were of high performance liquid chromatography (HPLC) grade or the highest grade available from Sigma. Methanol and tetrahydrofuran were Omnisolv grade, obtained from EMD Biosciences (San Diego, CA). Propan-2-ol was HPLC grade, and hexanes were optima grade, both obtained from Fisher.

Hydrolysis of Sphingolipids and Identification of Long-chain Bases

Sphingolipids were hydrolyzed using the method of Morrison and Hay (25) with modifications after Cahoon and Lynch (18). Briefly, solid samples (~100 mg) were freeze-dried, or samples in solvent were dried under nitrogen before adding 1 nmol of internal standard dissolved in methanol (d16:1 or d20:1; Matreya, Inc., Pleasant Gap, PA) followed by 1 ml of dioxane and 1 ml of 10% (w/v) barium hydroxide octahydrate in water. Samples were hydrolyzed for 16 h at 110 °C. After hydrolysis, 2 ml of 2% (w/v) ammonium sulfate was added to precipitate barium ions and to reduce the occurrence of a flocculent precipitate during subsequent derivatization, followed by 2 ml of diethylether. Samples were shaken, vortexed, and centrifuged to separate the phases. The upper phase was removed to a second tube, dried under nitrogen, and derivatized with *o*-phthaldialdehyde as previously described (26). Individual LCB species were separated by reversed phase HPLC using Agilent 1100 series pumps on a 4.6 × 250-mm XBD-C18 column (Agilent Technologies Inc., Palo Alto, CA). Elution was carried out at 1.5 ml/min with 20% solvent RA (5 mM potassium phosphate, pH 7), 80% solvent RB (100% methanol) for 7 min, increasing to 90% solvent RB by 15 min, followed by isocratic flow for 10 min before increasing to 100% solvent RB by 30 min with a 3-min 100% solvent RB wash before returning to 80% solvent RB and re-equilibrating for 2 min. Fluorescence was excited at 340 nm and detected at 455 nm.

Solubilization of Sphingolipids

Tissue was disrupted by grinding in liquid nitrogen with a mortar and pestle, and while still frozen, ~0.5 g fresh weight (fw), was transferred into a preweighed, precooled, Pyrex tube, after which the tube was weighed once more to determine the amount of tissue used. Sphingolipids were then extracted by four different methods.

Method I (after Bligh and Dyer (27))—To the frozen tissue, 2 ml of methanol, 1 ml of chloroform, and 0.35 ml of water were added. The sample was vortexed for 1 min before centrifuging at 500 × *g* for 10 min. The supernatant was removed to a second tube, and the pellet was extracted again with 1 ml of chloroform. After centrifuging as before, the supernatant was re-

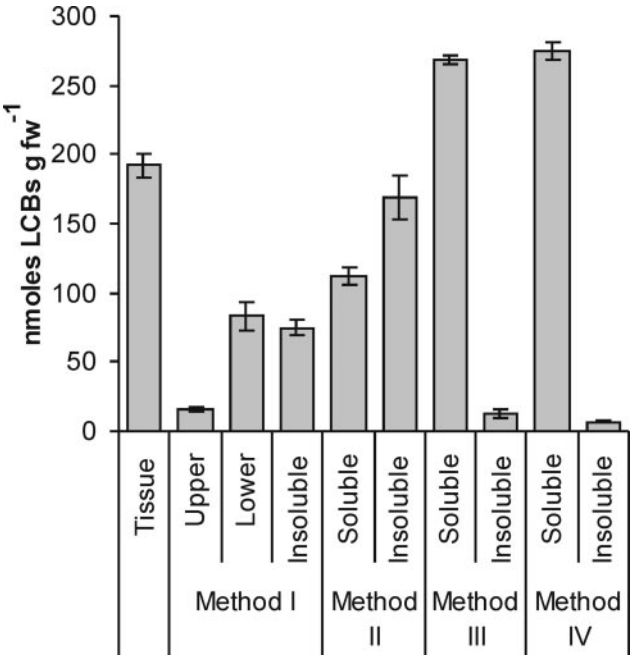

FIGURE 2. **Solubilization of sphingolipids from *Arabidopsis*.** The total amount of sphingolipid produced by hydrolysis of leaf tissue was calculated by integration and summation of the HPLC peaks compared with 1 nmol of spiked standard. This total is displayed in the *column labeled Tissue*. Four different extraction methods were used (Methods I–IV; see "Experimental Procedures" for details) to solubilize the sphingolipids (*Soluble*) from insoluble cell debris (*Insoluble*). The phase separation in Method I resulted in the soluble fraction being divided between an aqueous (*Upper*) and organic (*Lower*) phase. Exact numbers and LCB composition of each column are listed in Table 1.

moved and combined with the first. The insoluble material was retained for analysis. To the combined supernatants, 1 ml of 0.88% KCl in water was added. After vortexing for 1 min, the sample was spun as before to affect phase separation. The two phases were removed to fresh tubes and dried under nitrogen for analysis. Insoluble material present at the interphase was added to the pellet remaining after extraction and dried under nitrogen.

Method II (after Nichols (28) and Christie (29))—The frozen tissue was extracted with 50 ml of propan-2-ol by macerating for 1 min at 3000 rpm with an ULTRATURRAX T-25 fitted with a S25N-18G dispersing element. After centrifugation for 10 min at 500 × *g*, the supernatant was removed. The pellet was further extracted by shaking overnight with 50 ml of chloroform-propan-2-ol (1:1, v/v). After centrifugation as before, the supernatant was removed, combined with the previous extract, and dried under nitrogen for analysis.

Method III (after Hanson and Lester (30))—To the frozen tissue, 5 ml of solvent E (ethanol/water/diethylether/pyridine/ammonia (15:15:5:1:0.018, v/v/v/v/v)) was added. The tissue was transferred to a DUALL glass homogenizer and homogenized until fully disrupted. The sample was transferred back to a Pyrex tube, capped, and incubated at 60 °C for 15 min with occasional shaking. The extract was spun at 500 × *g* while still warm, and the supernatant was transferred to a fresh tube. The pellet was extracted twice more, each time with 5 ml of solvent E, and the supernatants were combined and dried under nitrogen for analysis.

TABLE 1

Solubilization of sphingolipids from *Arabidopsis thaliana*

Various procedures were used to solubilize sphingolipids (see "Materials and Methods"), and their effectiveness was measured by comparing the amount of sphingolipid present in the soluble phase and the insoluble material compared with the total (soluble + insoluble). Absolute values in nmol g fresh weight^{-1} ± S.D. are shown, and the calculated mol % of the total is shown in boldface type.

	t18:1(*Z*)	t18:1(*E*)	t18:0	d18:1(*Z*)	d18:1(*E*)	d18:0	Total
Total tissue	34.7 ± 2.2 **18%**	112 ± 5.5 **58%**	21.6 ± 1.4 **11%**	4.2 ± 0.2 **2%**	13.9 ± 1.4 **7%**	5.5 ± 0.2 **3%**	192 ± 8.6 **100%**
Method I							
Soluble (lower phase)	23.1 ± 2.7 **28%**	34.0 ± 4.8 **41%**	6.0 ± 1.0 **7%**	2.5 ± 0.3 **3%**	14.8 ± 2.0 **18%**	2.5 ± 0.5 **3%**	83.0 ± 10.7 **48%**
Soluble (upper phase)	0.91 ± 0.09 **6%**	10.4 ± 1.1 **68%**	2.2 ± 0.2 **14%**	0.04 ± 0.02 **0%**	0.89 ± 0.1 **6%**	0.96 ± 0.2 **6%**	15.4 ± 1.6 **9%**
Insoluble	7.32 ± 0.5 **10%**	53.0 ± 3.4 **71%**	10.0 ± 1.5 **13%**	0.19 ± 0.01 **0%**	2.5 ± 0.1 **3%**	1.8 ± 0.1 **2%**	74.9 ± 5.4 **43%**
Total	31.4 ± 2.9 **18%**	97.4 ± 6.1 **56%**	18.3 ± 1.8 **11%**	2.8 ± 0.3 **2%**	18.2 ± 2.1 **10%**	5.3 ± 0.6 **3%**	173 ± 12.4 **100%**
Method II							
Soluble	34.4 ± 2.1 **31%**	51.2 ± 5.0 **46%**	8.6 ± 0.8 **8%**	2.1 ± 0.08 **2%**	13.6 ± 0.49 **12%**	2.0 ± 0.1 **2%**	112 ± 6.5 **40%**
Insoluble	14.2 ± 0.58 **8%**	122 ± 12 **72%**	26.9 ± 2.6 **16%**	0.1 ± 0.0 **0%**	3.1±.17 **2%**	2.7 ± 0.4 **2%**	169 ± 15.6 **60%**
Total	48.6 ± 2.0 **17%**	173 ± 7.1 **62%**	35.5 ± 1.8 **13%**	2.24 ± 0.08 **1%**	16.6 ± 0.38 **6%**	4.72 ± 0.30 **2%**	281 ± 9.3 **100%**
Method III							
Soluble	48.7 ± 1.7 **18%**	167 ± 0.14 **62%**	32.3 ± 0.046 **12%**	1.8 ± 0.2 **1%**	13.9 ± 1.4 **5%**	4.9 ± 0.2 **2%**	268 ± 3.3 **96%**
Insoluble	1.5 ± 0.3 **12%**	8.0 ± 2.1 **64%**	2.6 ± 0.7 **21%**	0.0 ± 0.0 **0%**	0.17 ± 0.04 **1%**	0.17 ± 0.06 **1%**	12.5 ± 3.1 **4%**
Total	50.2 ± 1.6 **18%**	175 ± 2.2 **62%**	34.8 ± 0.75 **12%**	1.8 ± 0.2 **1%**	14.0 ± 1.4 **5%**	5.1 ± 0.2 **2%**	281 ± 6.4 **100%**
Method IV							
Soluble	50.8 ± .0005 **18%**	169 ± 4.5 **61%**	33.6 ± 1.5 **12%**	2.0 ± 0.01 **1%**	14.8 ± 0.32 **5%**	4.8 ± 0.06 **2%**	275 ± 6.3 **98%**
Insoluble	0.67 ± 0.06 **10%**	4.1 ± 0.4 **62%**	1.7 ± 0.1 **26%**	0.0 ± 0.0 **0%**	0.07 ± 0.01 **1%**	0.05 ± 0.00 **1%**	6.6 ± 0.6 **2%**
Total	51.5 ± 0.05 **18%**	173 ± 4.1 **61%**	35.3 ± 1.4 **13%**	2.0 ± 0.01 **1%**	14.9 ± 0.31 **5%**	4.8 ± 0.06 **2%**	282 ± 5.8 **100%**

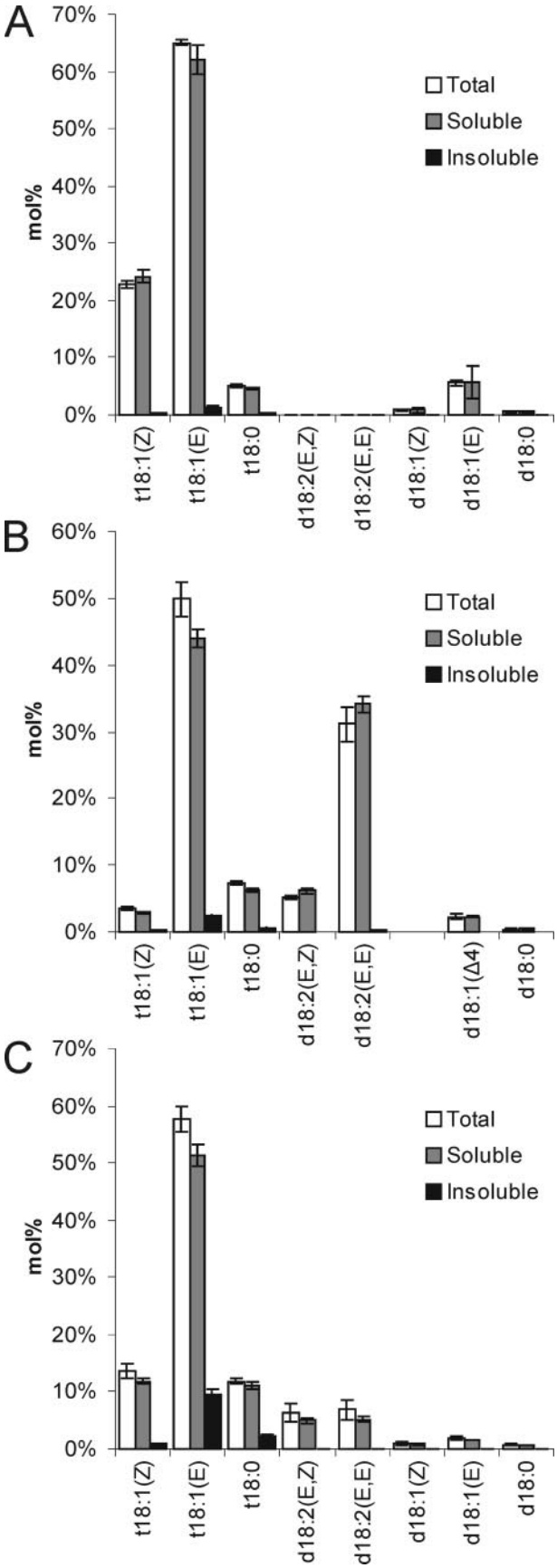

FIGURE 3. **Extraction efficiency of sphingolipid and LCB profiles from various plants.** The mol % of different LCBs in the sphingolipids of leaves from *Arabidopsis* (*A*), tomato (*B*), and soybean (*C*) was determined after hydrolysis of freeze dried tissue and HPLC quantitation (*Total*). The mol % of LCBs extracted (*Soluble*) and unextracted (*Insoluble*) created by the extraction procedure described under "Experimental Procedures" was determined as a percentage of the total amount of sphingolipid in both the soluble and insoluble fractions.

Method IV (after Toledo et al. (31))—The sample was processed exactly as for Method III, except 5 ml of solvent H was used (lower phase of propan-2-ol/hexane/water, 55:20:25 (v/v/v)) in place of solvent E.

Extraction of Sphingolipids

For separation of sphingolipids 3 g fresh weight of leaf tissue was placed in a 50-ml DUALL glass homogenizer to which 19.4 ml of propan-2-ol was added. The tissue was initially dispersed with an ULTRATURRAX T-25 fitted with a S25N-18G dispersing element at 3000 rpm until homogeneous. After dispersing, 5.8 ml of water and 1.8 ml of hexane were added, and the sample was further homogenized with the glass plunger of the DUALL homogenizer, attached to a Ryobi D45CK power drill rotating at up to 1000 rpm. When homogenization was complete, the sample was transferred to a 50-ml glass centrifuge tube, capped, and incubated at 60 °C for 15 min. After centrifugation at 500 × *g* for 10 min, the supernatant was decanted to a second tube, and the pellet was extracted twice more with 10 ml of solvent H, incubating at 60 °C for 15 min each time. The supernatants were combined after each extraction and finally dried under nitrogen.

Solid Phase Extraction of Sphingolipid Extract

The dried lipid extract was dissolved by the sequential addition of 1 ml of tetrahydrofuran, 1 ml of methanol, and 1 ml of water with vortexing and sufficient sonication to effect solubilization after each addition. A 100-μl aliquot was removed for hydrolysis and analysis (Total Extract). A SepPak Plus C18 cartridge (Waters, Milford, MA) was prepared by fitting a glass 6-ml syringe with Teflon frit (Supelco, Bellefonte, PA) to the inlet and passing 2 ml of methanol and 2 ml of methanol/water (1:1, v/v) through the cartridge. After the addition to the sample of 300 mg of Hyflo SuperCel (Avocado Research Chemicals Ltd., Lancastershire, UK) and 2 ml of water, the sample was vortexed, rapidly poured onto the cartridge, and allowed to drain by gravity flow. The column was rinsed twice with 2 ml of methanol/water (1:1, v/v), and the flow-through and rinse were combined and saved for analysis. The sample was eluted sequentially with 1 ml of methanol; 1 ml of chloroform; 2 ml of chloroform/methanol (1:1, v/v) containing 0.01% triethylamine and 2 ml of chloroform, methanol, 1.85% trimethylamine in water (16:16:5 v/v/v); and 4 ml of chloroform/methanol/water/ammonia (16:16:4:1, v/v/v/v). The eluate was dried under nitrogen and redissolved in 2.9 ml of chloroform/methanol/water (16:16:5, v/v/v) from which a 100-μl aliquot was removed for analysis (anion exchange load).

The C18 eluate was applied to 2 ml of AG4X-X4 acetate resin (Bio-Rad) supported in a 6-ml glass syringe with upper and lower Teflon frit and allowed to flow by gravity. The column was washed with chloroform/methanol/water (16:16:5, v/v/v) until the eluate ran clear. The column flow-through (neutral

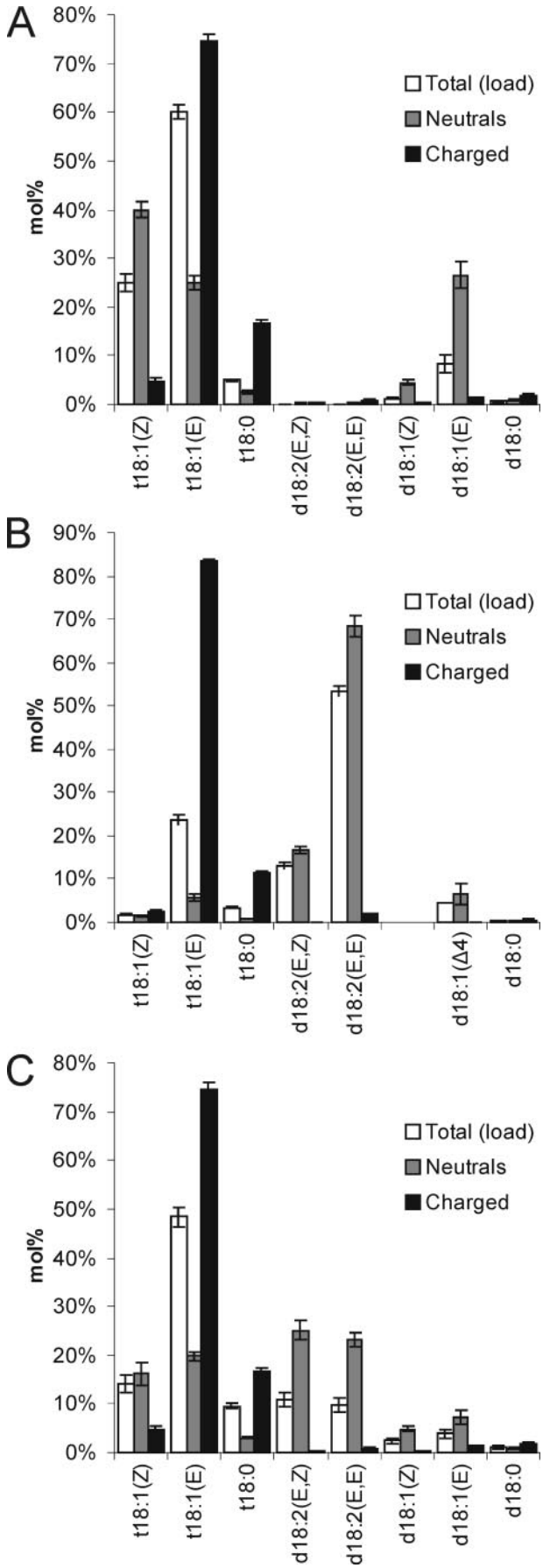

lipids) was dried under nitrogen and redissolved in 2.8 ml of chloroform/acetic acid (99:1), and 100 μl was removed for analysis. The anionic charged lipids were eluted from the column with 6 ml of chloroform/methanol/water/ammonia (16:16:5:1) containing 0.1% triethylamine. The eluate (anionic lipids) was dried under nitrogen and redissolved in 280 μl of propan-2-ol/hexane/water (3:1:1, v/v/v), and 10 μl was removed for analysis.

The neutral fraction was applied to a SepPak Silica cartridge equilibrated with chloroform/acetic acid (99:1, v/v) and allowed to drain by gravity flow. The cartridge was washed with 15 ml of chloroform/acetic acid (99:1, v/v), which was discarded. Sphingolipids were sequentially eluted with 4 ml of acetone and 4 ml of methanol, dried under nitrogen, and redissolved in 300 μl of chloroform and stored at −30 °C for HPLC analysis.

Preparative HPLC of Anionic Sphingolipids

The charged lipid fraction was separated by injecting 40 μl of lipid onto a 4.6 × 250-mm Xpertek Spherisorb silica HPLC column (Cobert Associates, Saint Louis, MO) at a column temperature of 50 °C and a flow rate of 1 ml min^{-1} using a gradient of 100% solvent SA (propan-2-ol/hexane/water/acetic acid (60:35:4:1 v/v/v/v) containing 5 mM ammonium acetate), 0% solvent SB (propan-2-ol/water/acetic acid (60:39:1, v/v/v) containing 5 mM ammonium acetate) for 5 min increasing to 25% solvent SB by 10 min and continuing at 25% until 20 min, followed by an increase to 100% solvent SB by 30 min. The column was washed with 100% solvent SB for 3 min before returning to 0% solvent SB over 1 min and re-equilibrating with 100% solvent SA for 10 min. Fractions were collected every 1 min starting at 2 min after sample injection.

Preparative HPLC of Neutral Sphingolipids

The neutral lipid fraction was separated by injecting 40 μl of lipid onto a 4.6 × 250-mm Xpertek Spherisorb silica-amino HPLC column (Cobert Associates) at a column temperature of 25 °C and a flow rate of 1 ml min^{-1} using a gradient of 100% solvent NA (acetonitrile/methanol/acetic acid (97:2:1, v/v/v) containing 5 mM ammonium acetate), 0% solvent NB (methanol/acetic acid (99:1, v/v) containing 5 mM ammonium acetate) for 3 min, increasing to 100% solvent NB by 23 min. The column was washed with 100% solvent NB for 4 min before decreasing the solvent to 0% solvent NB over 2 min and re-equilibrating with 100% solvent NA for 3 min. Fractions were collected every 1 min starting at 2 min after sample injection.

Electrospray Ionization and Mass Spectrometry of Sphingolipids

Fractions containing sphingolipid were infused into the TurboV electrospray source of an API 4000 mass spectrometer

FIGURE 4. **Anion exchange separation of sphingolipid classes.** Samples for anion exchange from *Arabidopsis* (*A*), tomato (*B*), and soy bean (*C*) were desalted by loading onto a C18 cartridge, washing, and eluting to produce the desalted extract. An aliquot was removed and analyzed for LCB content (*Total (load)*). The remainder of the extract was applied to an AG4-X4 (acetate form) anion exchange column. An aliquot of the column flow-though and wash was analyzed for LCB content (*Neutrals*). The sphingolipids that bound to the column were eluted, and an aliquot was analyzed for LCB content (*Charged*).

TABLE 2

Purification of sphingolipids from *Arabidopsis*

Each step of the purification procedure was monitored for LCB content, which was calculated as nmol g fw^{-1} and averaged between four samples. Data from the HPLC fractions identified as containing specific sphingolipids were summed together to produce the total for that particular sphingolipid. The mol % of each type of LCB is shown in boldface type. The percentage yield for each step of the purification is underlined in the Total column. Total tissue is set to 100%.

Arabidopsis	t18:1(8Z)	t18:1(8E)	t18:0	d18:1(8Z)	d18:1(8E)	d18:0	Total
Total tissue	59.8 ± 2.9	170.5 ± 9.0	13.5 ± 0.9	2.1 ± 0.3	14.7 ± 1.9	1.4 ± 0.2	262.0 ± 14.3
	22.8%	**65.1%**	**5.2%**	**0.8%**	**5.6%**	**0.5%**	100%
Total extract	30.9 ± 1.2	88.9 ± 3.6	7.2 ± 0.6	2.2 ± 0.4	14.8 ± 1.4	1.3 ± 0.2	145.4 ± 3.8
	21.3%	**61.1%**	**5.0%**	**1.5%**	**10.2%**	**0.9%**	55.5%
Anion exchange: load	47.3 ± 17.8	111.6 ± 34.5	9.0 ± 2.4	2.2 ± 0.7	14.9 ± 4.4	1.2 ± 0.2	186.1 ± 59.2
	25.0	**60.0%**	**4.9%**	**1.2%**	**8.2%**	**0.7%**	71.0%
Neutral sphingolipids	13.0 ± 2.2	8.2 ± 1.3	0.8 ± 0.2	1.5 ± 0.2	8.6 ± 1.2	0.3 ± 0.0	32.6 ± 4.5
	39.9%	**25%**	**0.1%**	**4.5%**	**26.6%**	**0.9%**	12.4%
Anionic sphingolipids	7.3 ± 2.1	67.0 ± 19.3	4.8 ± 0.9	0.1 ± 0.0	2.9 ± 0.4	1.1 ± 0.4	83.2 ± 23.0
	8.7%	**80.4%**	**5.9%**	**0.1%**	**3.6%**	**1.3%**	31.8%
Ceramide	0.04	0.68	0.66	0	0	0	1.37
	2.9%	**49.3%**	**47.7%**	**0%**	**0%**	**0%**	0.5%
Glucosylceramide	10.9	8.8	0.3	0.5	6.1	0.1	26.7
	40.9%	**32.9%**	**1.1%**	**2.0%**	**22.7%**	**0.4%**	10.2%
GIPC	3.6	36.5	7.4	0	1.3	1.3	50.1
	7.3%	**72.8%**	**14.7%**	**0%**	**2.5%**	**2.7%**	19.1%

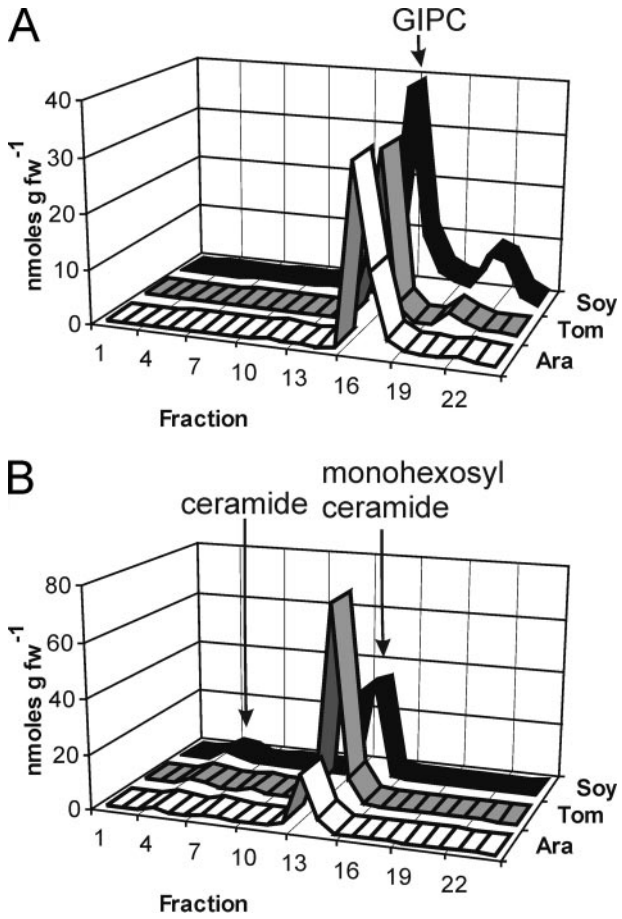

FIGURE 5. **HPLC separation of sphingolipids.** Sphingolipids from each class, charged (*A*) and neutral (*B*) were separated by normal phase HPLC, and fractions were collected. Each fraction was analyzed for LCB content, and the total LCB in each fraction was calculated on a g fw^{-1} basis. This was plotted against fraction number to indicate the elution of sphingolipids from the HPLC column. *Soy*, soybean; *Tom*, tomato; *Ara*, Arabidopsis.

(Applied Biosystems, Foster City, CA) using the flow from a KDS100 syringe pump (KD Scientific Inc., Holliston, MA) at 10 μl min^{-1} with a needle temperature of 100 °C, curtain gas 10, gas1 20 and gas2 0, needle voltage +5000 V, and declustering potential 100 V. Collision energy was adjusted on a compound-dependent basis.

RESULTS

Assay for Sphingolipids—A prerequisite for purification of any compound is an ability to measure it both qualitatively and quantitatively. Sphingolipids are unique compared with other lipids, since each molecule contains a 2-aminooctadecane backbone or LCB. Hence, hydrolysis and measurement of the liberated LCBs is a quantitative measure of the sphingolipid content. LCBs were liberated by hydrolyzing the sphingolipids under conditions that minimized the formation of artifacts (18, 25), permitted good separation and quantification of the products (Fig. 1), and could be performed with minimal sample handling and cleanup. The identity of each peak was assigned by the following: (*a*) comparison with known standards (t18:0, d18:1(4*E*), and d18:0); (*b*) mass spectrometry (t18:1, t18:0, d18:2, d18:1-Glc, d18:1, 1,4-*anhydro*-t18:1, and d18:0); (*c*) inference from elution time (t18:1-Glc, d18:2-Glc, 1,4-*anhydro*-t18:0, and *E*/*Z* isomers); and (*d*) comparison with previously published data (4, 19, 32). The hydrolysis reaction was found to be essentially complete by 8 h, although overnight hydrolysis was usually more convenient, but became increasingly nonlinear with respect to the amount of starting material at values greater than 10 mg dry weight (data not shown). Consequently, the equivalent of 10 mg dry weight (~100 mg fresh weight) was used for the majority of analyses.

Solubilization of Sphingolipids—Previous studies have shown that standard lipid extraction techniques are poor at solubilizing plant sphingolipids (4, 24). Hydrolysis of total tissue samples from *Arabidopsis* indicated a sphingolipid content of 192 ± 8.5 nmol g fw^{-1} (Fig. 2 and Table 1). Measurement of sphingolipids in Method I (see "Experimental Procedures") showed that 43% of the total sphingolipids remained insoluble, with the soluble fraction divided between 48% in the lower chloroform phase and 9% in the upper aqueous phase. The total amount of sphingolipids recovered was 173 ± 12 nmol g fw^{-1}. Method II, based around extraction of lipids into large volumes of propan-2-ol to inhibit lipases, solubilized 40% of the total sphingolipids. The total amount of sphingolipids measured in this instance was 281 ± 9 nmol g fw^{-1}. Method III used a basic, hydrophilic solvent containing substantial amounts of water that was developed for the extraction of

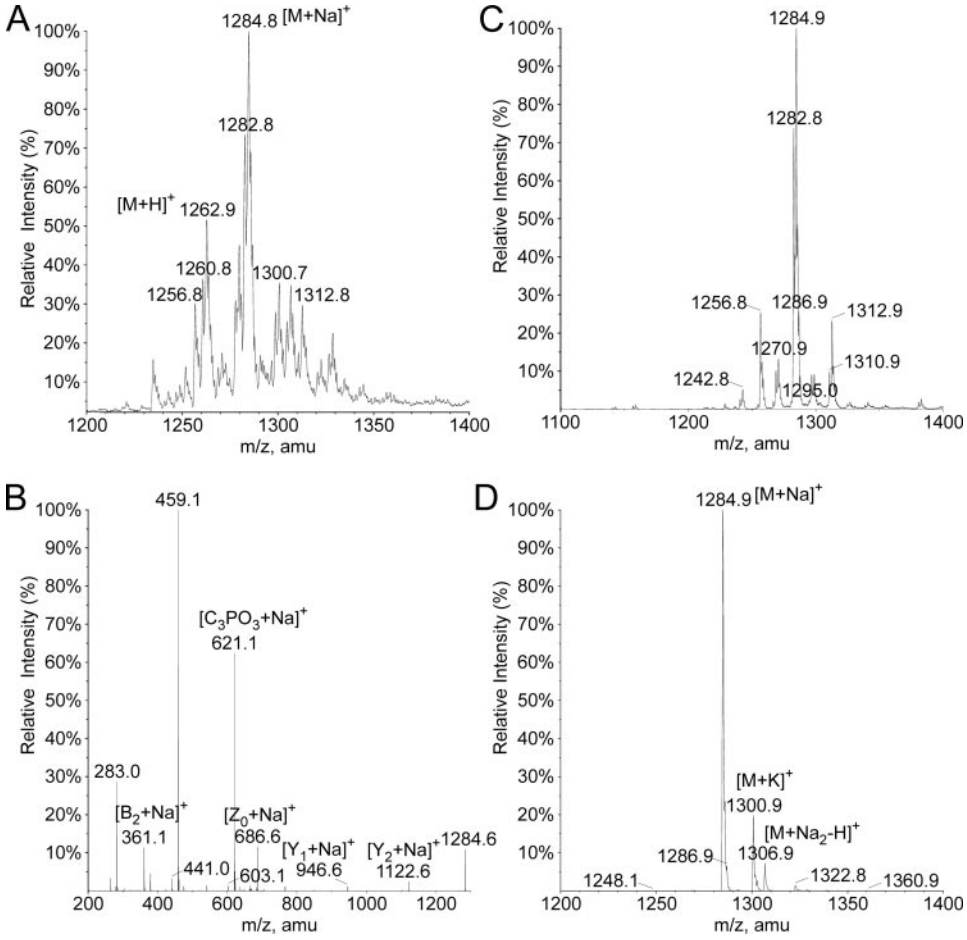

FIGURE 6. **Mass spectra of *Arabidopsis* GIPC.** *A*, simple mass spectrum of fraction 16 from HPLC of *Arabidopsis* charged sphingolipids. Subsequently identified adducts are labeled. *B*, enhanced product ion mass spectrum of *m/z* 1284.8; major and important fragments are labeled. *C*, mass spectrum obtained in precursor ion scan mode with *m/z* 621 as the product ion showing the variation in mass associated with varying ceramide backbones. *D*, mass spectrum obtained in neutral loss scan mode with *m/z* 664 as the neutral fragment lost. Adduct ions are labeled.

inositolphosphoceramides from yeast (30). A similar solvent mix has also been used to extract phosphoinositol-containing sphingolipids from plants (21). Using this solvent, 96% of the 281 ± 6 nmol g fw^{-1} of sphingolipid measured could be solubilized, indicating that a relatively small proportion of sphingolipids are unextractable. Method IV, based upon a mix of propan-2-ol, water, and hexane, was equally efficient, extracting 98% of the 282 ± 6 nmol g fw^{-1} of sphingolipid and was the preferred method for extracting sphingolipids for purification due to the presence of lipase inhibiting propan-2-ol and the neutral pH of the solvent. The efficacy and general applicability of the extraction method was tested by extracting sphingolipids from leaf tissue of *Arabidopsis*, tomato, and soybean (Fig. 3), where the total amount of sphingolipid solubilized was 98, 96, and 87% of the total in each species, respectively. These data indicate that propan-2-ol/hexane/water mixes may be useful and efficient in extracting sphingolipids from a broad range of samples.

Separation of Neutral and Charged Sphingolipids—A clear functional division between the classes of plant sphingolipids is the presence or absence of a charged head group. Ion exchange chromatography has been used to purify phosphoinositol-containing sphingolipids from yeast (33), and this was adapted to the plant extracts. In all three species examined, an enrichment of different LCBs was found in each of the lipid classes. In each species, the anionic sphingolipids consisted of >95% trihydroxy LCBs, with the majority of that as t18:1(8*E*) (Fig. 4 and Table 2). The neutral fractions contained more variation between species with regard to LCB content. The neutral sphingolipids from *Arabidopsis* contained mostly t18:1 LCBs (65%) with a greater proportion of t18:1(8*Z*) than t18:1(8*E*). The neutral sphingolipids from tomato contained almost entirely d18:2 (>80%), with almost 4 times as much d18:2(4*E*/8*E*) as d18:2(4*E*/8*Z*). In contrast, soybean neutral sphingolipids were divided between t18:1 (39%) and d18:2 (48%) with approximately equal ratios of Δ8 *E* and *Z*.

HPLC Separation of Sphingolipids—In order to discern how many different species of sphingolipid were present in each class of neutral and anionic lipids, the lipids were separated by normal phase HPLC, from which fractions were collected and analyzed for sphingolipid content (Fig. 5). Both the anionic and neutral sphingolipid classes contained one major sphingolipid. Neutral sphingolipids were identified as ceramide, 2-hydroxy-ceramide, and monohexosylceramide by comparison with purified standards. Mass spectra of the purified neutral sphingolipids matched the existing mass spectra for these compounds and that of the standards. No standards exist for GIPCs, however, and the nature of these compounds was investigated by mass spectrometry.

Electrospray Ionization/Mass Spectrometry of Charged Plant Sphingolipids—Sphingolipids are a diverse class of compounds containing multiple LCBs and fatty acids with varying degrees of saturation and hydroxylation. Fatty acids usually differ by 2 carbon units with an *m/z* of 28; hence, sphingolipids were identified in each sample as a group of compounds that differed by an *m/z* of 28. In each case, the fractions containing the majority of the charged sphingolipids (fractions 16 and 17) were infused into the mass spectrometer and a profile typical for sphingolipids identified (Figs. 6*A* and 7*A*). The fragmentation scheme for GIPCs is shown in Fig. 8.

From *Arabidopsis*, the major parent ion detected was *m/z* 1284.8 $[M + Na]^+$ (Fig. 6*A*). Product ion scans of this ion created a major product ion of *m/z* 621.1 and *m/z* 459.1 with lesser fragments of *m/z* 361.1 and *m/z* 283.0 (Fig. 6*B*). Precursor ion scans for

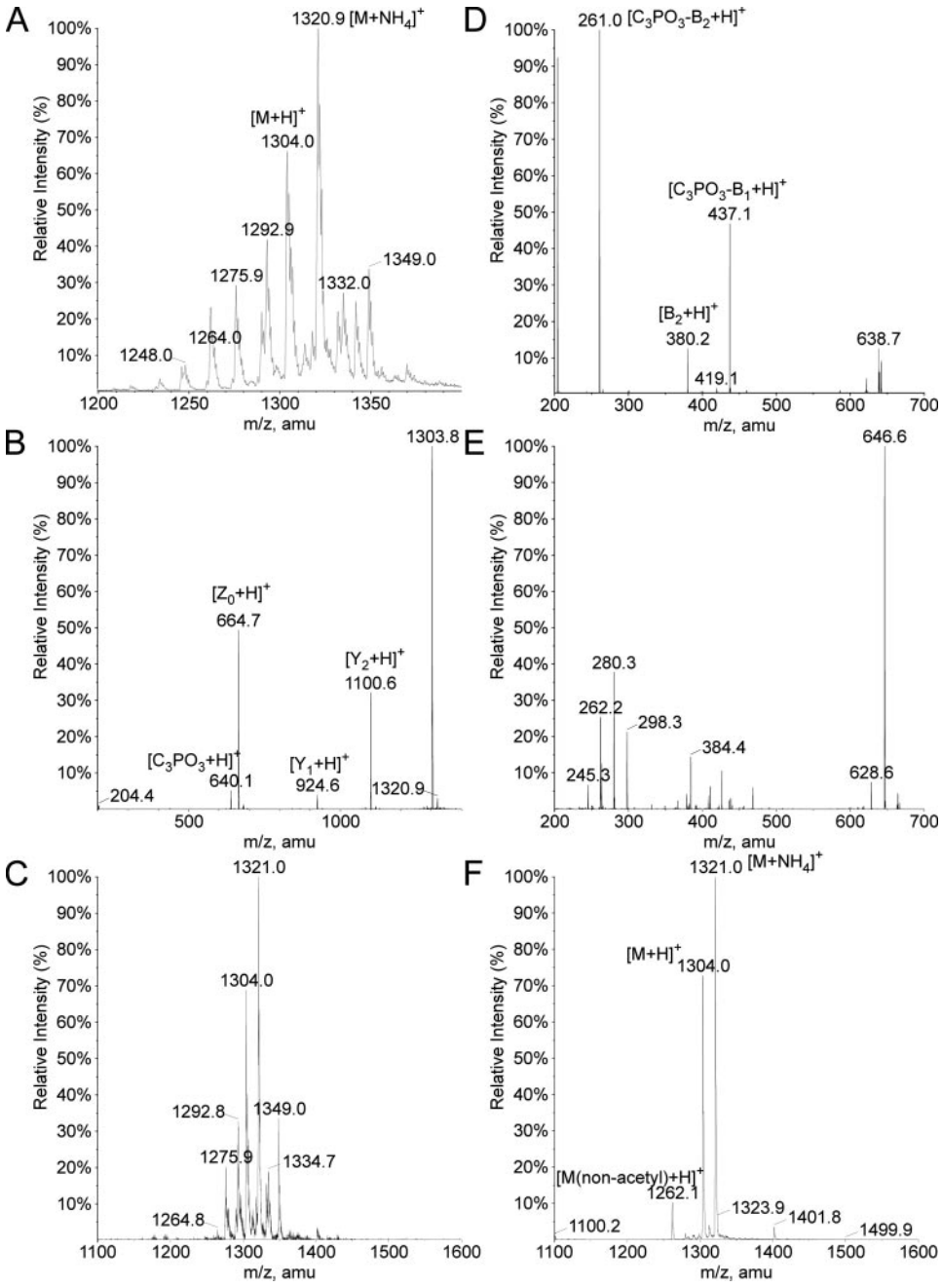

FIGURE 7. **Mass spectra of tomato GIPC.** *A*, simple mass spectrum of fraction 16 from HPLC of tomato charged sphingolipids. Subsequently identified adducts are labeled. *B*, product ion mass spectrum of *m/z* 1321. Important fragments are labeled. *C*, mass spectrum acquired in precursor ion scan mode with *m/z* 640.1 as the product ion. *D*, mass spectrum acquired in MS3 mode resulting from additional fragmentation of the *m/z* 640.1 fragment ion. *E*, mass spectrum acquired in MS^3 mode resulting from additional fragmentation of the *m/z* 664.6 fragment ion (see Fig. 9 for interpretation). *F*, mass spectrum acquired in precursor ion scan mode with *m/z* 664.6 as the product ion. Adduct and nonacetylated ions are labeled.

m/z 621.1 revealed six sphingolipid species with varying acyl-chain length and degrees of desaturation, indicating that the *m/z* 621.1 ion represents a common head group fragment (Fig. 6*C*). The fragmentation of *m/z* 1284.8 to *m/z* 621.1 represents a neutral loss of 663.7 atomic mass units (Z_0 fragment) and this can be seen as a minor $[Z_0 + H]^+$ species at *m/z* 664.7 in the product ion scan (Fig. 6*B*). This neutral loss corresponds to the molecular weight of t18:1h24:0 ceramide (*N*-2-hydroxylignoceroyl-8-phytosphingenine) and is the major ceramide backbone in the charged sphingolipids. Neutral loss scans for loss of 664 found one major species at *m/z* 1284.9 $[M + Na]^+$ and additional adduct species at *m/z* 1300.9 $[M + K]^+$ and *m/z* 1306.9 $[M + Na_2]^+$ (Fig. 6*D*). Using the information provided from these scans, the molecular structure of the major charged sphingolipid from *Arabidopsis* was proposed to be hexose-hexuronic-inositol-phosphoceramide (Fig. 8). The exact identity of the hexose and hexuronic acid could not be assigned based on the mass spectrum. The atomic masses corresponding to particular fragments are tabulated in Table 3.

Mass spectrometry of the equivalent fraction from tomato revealed that the major charged sphingolipid in tomato is not the same as in *Arabidopsis*. The major peak was at *m/z* 1320.9 with an associated pattern of peaks at 28 atomic mass units difference (Fig. 7*A*). The product ion spectrum of *m/z* 1321 showed that the *m/z* 1304 ion is rapidly generated from the *m/z* 1320.9 ion, corresponding to the loss of an ammonium adduct (*m/z* 17). Two other fragments at *m/z* 664.7 and *m/z* 640 are potentially the ceramide and head group, respectively (Fig. 7*B*). Precursor ion scans of the *m/z* 640 fragment reveal a cluster of ions separated by 28 atomic mass units, indicating that this is the head group fragment (Fig. 7*C*). MS^3 of the *m/z* 640 ion produced a spectrum consistent with a parent ion structure *N*-acetylhexosamine-hexuronic acid-inositolphosphoceramide (Fig. 7*D*). MS^3 of the *m/z* 664.7 fragment established this as the t18:1-h24:0 ceramide backbone (Figs. 7*E* and 9). Precursor ion scans with the *m/z* 664.7 fragment revealed the major peaks at *m/z* 1321.0 as expected and additional peaks at *m/z* 1304.0 and 1262.1 (Fig. 7*F*). This is consistent with the *m/z* 1321.0 peak being an ammonium adduct $[M + NH_4]^+$, the *m/z* 1304 peak being the protonated ion $[M + H]^+$ and the *m/z* 1262.1 peak the nonacetylated hexosamine- hexuronic-inositol-phosphoceramide.

Fraction 16 from soybean produced identical results to tomato (data not shown). The soybean HPLC profile also showed a significant amount of a second charged sphingolipid peak in fraction 22. Mass spectrometry identified numerous

compounds in this fraction, but none were pure enough for conclusive identification. In light of this, reexamination of fraction 22 from the HPLC of *Arabidopsis* anionic sphingolipids revealed a species with an *m*/*z* of 1447 that lost *m*/*z* 664, consistent with a dihexosyl-hexuronic-IPC species, but the signal was too weak to obtain conclusive spectra (data not shown).

Quantification of Sphingolipid Classes—In theory, it should be possible to separate the sphingolipid classes and quantify the differing amounts in each class, thereby determining the relative proportions in the original tissue. In practice, however, losses occur during the separation process, which, without the addition of internal standards for each compound at the start of the separation, makes absolute quantification impossible. The relative proportion of each class may be calculated based on the quantification of each sphingolipid peak, however (Table 3), and for *Arabidopsis* this was calculated to be ceramide 1.7%, monohexosylceramide 33.9%, and GIPC 64.4%, making GIPCs the predominant sphingolipid. This percentage is only valid assuming equal losses of each class of compound during the procedure, which does not appear to be the case. Due to the unique distribution of LCBs between the classes, selective losses from one class relative to another cause a change in the molar ratio of the LCB content. This can be seen most dramatically in the tomato and soybean sphingolipid samples (compare totals in Figs. 3 and 4), where the steps involved had been optimized only for *Arabidopsis*, leading to greater losses from the tomato and soybean samples. Calculation of the proportion of monohexosylceramide to GIPC using the different ratios of t18:1(8*Z*) and t18:1(8*E*) in these separated sphingolipids compared with the ratio in total tissue yields a sphingolipid composition of monohexosylceramide 37% and GIPCs 63%. Calculation based on the proportions of t18:1 *E* to *Z* in the crude neutral and anionic fractions gives a similar composition of monohexosylceramides 31% and GIPCs 69%. Allowing for the experimental errors involved, these data indicate that, in *Arabidopsis*, GIPCs are mole for mole approximately twice as abundant as monohexosylceramides.

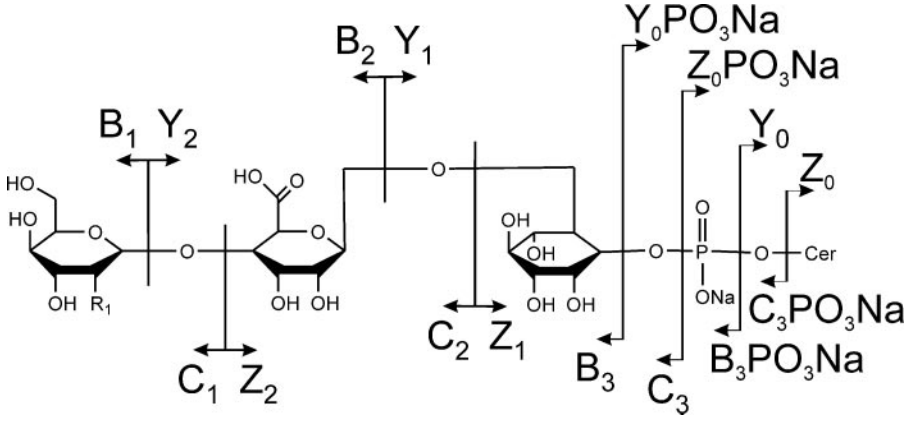

FIGURE 8. **Characteristic fragmentations of GIPCs.** Standard nomenclature for fragmentation of glycolipids (36) and GIPCs (35, 37) applied to the plant GIPCs reported in this study. All hydrogen transfers associated with fragmentation are assumed. Hexose conformers and linkages are arbitrary. Group R_1 represents a hydroxyl in *Arabidopsis* or an (acetyl) amine in tomato and soybean. Observed fragments and theoretical masses are paired in Table 3.

DISCUSSION

Plant sphingolipids are receiving increased attention due to the recognition of their roles in a number of fundamental plant processes. Given the large amount of data on sphingolipids in animals and yeast, it is only reasonable to make comparisons between these two systems and plants to look for similarities. Caution needs to be exercised when making such comparisons if the exact sphingolipid content of the organism of interest is unknown, since organisms may vary substantially in their sphingolipid classes and LCB profile.

TABLE 3

Diagnostic ESI-MS/MS fragments for plant GIPCs

Shown are the ions produced by the fragmentation of GIPCs according to the scheme in Fig. 6. Theoretical exact *m*/*z* values were calculated based on predicted structural fragmentations. Observed ions in the mass spectra were matched to theoretical fragments, and the observed *m*/*z* values are indicated in parentheses.

Diagnostic fragment	Arabidopsis: theoretical *m*/*z* (detected *m*/*z*)	Diagnostic fragment	Tomato/Soybean: theoretical *m*/*z* (detected *m*/*z*)
$[M + Na]^+$	1284.7 (1284.8)	$[M + Na]^+$	1325.7 (1326.0)
$[M + H]^+$	1262.7 (1262.9)	$[M + NH_4]^+$	1320.8 (1320.9)
$[Y_2 + Na]^+$	1122.6 (1122.6)	$[M + H]^+$	1303.8 (1304.0)
$[Z_2 + Na]^+$	1104.7 (1104.6)	$[Y_2 + NH_4]^+$	1117.7 (1117.6)
$[Y_1 + Na]^+$	946.6 (946.6)	$[Y_2 + H]^+$	1100.7 (1100.6)
$[Z_1 + Na]^+$	928.6 (928.7)	$[Z_2 + H]^+$	1082.7 (1082.8)
$[Y_0PO_3 + Na]^+$	784.6 (784.6)	$[Y_1 + NH_4]^+$	941.7 (941.7)
$[Z_0PO_3–H_2 + Na]^+$	766.6 (766.6)	$[Y_1 + H]^+$	924.7 (924.6)
$[Y_0 + Na]^+$	704.6 (704.6)		
$[Z_0 + Na]^+$	686.6 (686.6)	$[Z_0 + NH_4]^+$	681.7 (681.9)
$[Z_0 + H]^+$	664.6 (664.7)	$[Z_0 + H]^+$	664.6 (664.7)
$[C_3PO_3 + Na]^+$	621.1 (621.1)	$[C_3PO_3 + H]^+$	640.1 (640.1)
$[B_3PO_3–H_2 + Na]^+$	603.1 (603.1)	$[C_3PO_3–H_2O + H]^+$	622.1 (622.2)
$[C3 + Na]^+$	541.1 (541.2)		
$[B_3 + Na]^+$	523.1 (523.1)		
$[C_3PO_3–B_1 + Na]^+$	459.1 (459.1)	$[C_3PO_3–B_1 + H]^+$	437.1 (437.1)
$[C_3PO_3–C_1 + Na]^+$	441.0 (441.0)	$[C_3PO_3–B_1–H_2O + H]^+$	419.1 (419.1)
$[C_2 + Na]^+$	379.1 (379.1)		
$[B_2 + Na]^+$	361.1 (361.1)	$[B_2 + H]^+$	380.1 (380.2)
$[C_3PO_3–B_2 + Na]^+$	283.0 (283.0)	$[C_3PO_3–B_2 + H]^+$	261.0 (261.0)
$[C_3PO_3–B_2 + Na]^+$	265.0 (265.0)	$[C_3PO_3–C_2 + H]^+$	243.0 (243.0)
$[C_1 + Na]^+$	203.1 (203.1)	$[B_1 + H]^+$	204.1 (204.1)

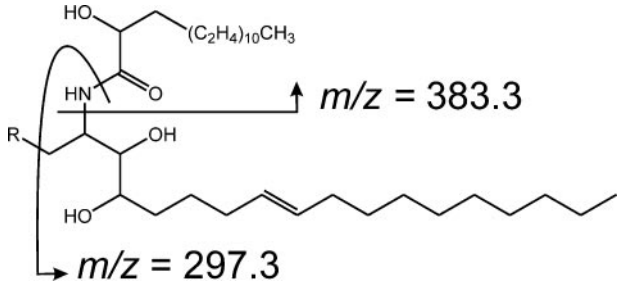

FIGURE 9. **Fragmentation of the ceramide from GIPCs.** Fragmentation of ceramide from GIPCs produces two major products, depending on which side of the amide bond the fragmentation occurs. Both fragments are readily observable in MS^3 spectra (Fig. 7*E*) with additional fragmentation of the LCB ion caused by dehydration.

In this respect, plants are uniquely different from animals and yeast in that the major LCBs t18:1(8*E*/*Z*) and d18:2(4*E*/(*E*/*Z*)) are not found in these organisms. The proportion of d18:2 found in a particular species appears to segregate along taxonomic lines, with the *Solanacae* (tomato and tobacco) having large proportions of d18:2, the *Fabacae* (pea and soybean) an intermediate amount of d18:2, and the *Brassicacae* very low to nonexistent levels of d18:2 (*Arabidopsis* and other brassicas). This may be a reflection of a difference in Δ4 desaturase activity between the different taxonomic groups. Indeed, all d18:1 in tomato contained the Δ4 desaturation in contrast to soybean and *A. thaliana*, where little or no d18:1 Δ4 was detected respectively. In all cases examined, the d18:2 appears largely confined to the glucosylceramide fraction. The functional significance of this division remains to be assessed.

A more striking division of the LCBs and one that appears to be conserved between species is the high level of trihydroxy-LCBs in the GIPCs. The uniformity of this feature in the face of diversity in other sphingolipid classes suggests a conserved functional role for the 4-hydroxy of the LCB in GIPCs. Interestingly, the ceramide fraction of neutral lipids is also highly enriched in trihydroxy-LCBs with a t18:1(8*E*) to 18:1(8*Z*) ratio similar to GIPCs. This is consistent with free ceramide originating from GIPC hydrolysis, suggesting that GIPCs are turned over much faster than glucosylceramides. Consistent with this, labeling of tomato sphingolipids by feeding labeled serine to leaf discs almost exclusively labels GIPCs and not monohexosylceramides (34). The significance of the increased turnover of GIPCs is not known but may be a result of their recycling between the Golgi apparatus and the plasma membrane, where they are apparently enriched (4).

Solubilization of sphingolipids has been a major obstacle to their study. Most lipid extraction techniques utilize extraction into chloroform/methanol mixes and phase partition into chloroform to remove nonlipid contaminants. This does not work well for sphingolipids with large amounts of GIPCs unextracted from the insoluble tissue. Extraction into chloroform-methanol-water mixes is possible if the water content is high. A ratio of 16:16:5 (v/v/v) proves an excellent solvent for GIPCs; however, upon phase partition, the GIPCs become distributed between the chloroform and aqueous phases and the interphase precipitate. A solvent mixture based on propan-2-ol, water, and hexane was finally chosen, because the primary alcohol is known to inhibit lipases and the mixture is relatively innocuous, making handling easier. Sphingolipids are thought to have a higher phase transition temperature than other lipids and are traditionally extracted at higher temperatures; 60 °C used in this study did not affect the lipids themselves and gave adequate solubilization. The vital components of the sphingolipid extraction procedure are effective cell disruption through the use of a close fitting glass homogenizer, the use of solvents containing a significant proportion of water, and incubation at high temperature.

The GIPC class of sphingolipids from *Arabidopsis* consists of just one major species, hexose-hexuronic-inositolphosphoceramide. Under the conditions used here, it naturally formed a sodium adduct in electrospray ionization-mass spectrometry, although no sodium was added to the sample and ammonium acetate was present in the solvent. Previous characterization of GIPCs from fungi has shown that increased sensitivity can be achieved by forming lithium adducts (35). Attempts to displace the sodium by adding lithium iodide or lithium acetate failed to produce significant amounts of lithium adduct up to 5 mM final concentration, and higher concentrations caused ion suppression, indicating a high affinity of the *Arabidopsis* GIPC for sodium. Despite this, fragmentation and identification of the sodium adduct fragments was possible, although the presence of additional potassium and disodium adducts may represent a complicating factor for future quantification of these lipids by electrospray ionization-tandem mass spectrometry.

The major GIPCs from soybean and tomato behaved quite differently from the *Arabidopsis* GIPC naturally forming ammonium or hydrogen adducts, presumably due to the difference in structures of the GIPCs between these species. In all cases, the plant GIPCs appear to most readily fragment at the Z_0 position, which requires MS^3 to extract further information about the ceramide backbone. This can easily be achieved by MS^3 in the Q-TRAP 4000 or by setting the declustering potential high enough to cause in-source fragmentation of the parent ion followed by conventional tandem mass spectrometry (35).

In summary, procedures necessary to determine the sphingolipid content of a target, model plant species, in this case *A. thaliana*, have been established, and it has been shown that they are generally applicable to other species. This will provide the opportunity to establish an *Arabidopsis* sphingolipidomics program for separating and identifying all of the major sphingolipid species. Future high-throughput screening procedures should enable detailed characterization of sphingolipid and sphingolipid signaling mutants and increase our understanding of the role of sphingolipids in *Arabidopsis*.

REFERENCES

1. Dickson, R. C., and Lester, R. L. (2002) *Biochim. Biophys. Acta.* **1583,** 13–25
2. Dunn, T. M., Lynch, D. V., Michaelson, L. V., and Napier, J. A. (2004) *Ann. Bot.* (*Lond.*) **93,** 483–497
3. Futerman, A. H., and Hannun, Y. A. (2004) *EMBO Rep.* **5,** 777–782
4. Sperling, P., Franke, S., Luthje, S., and Heinz, E. (2005) *Plant Physiol. Biochem.* **43,** 1031–1038
5. Borner, G. H. H., Sherrier, D. J., Weimar, T., Michaelson, L. V., Hawkins, N. D., MacAskill, A., Napier, J. A., Beale, M. H., Lilley, K. S., and Dupree, P. (2005) *Plant Physiol.* **137,** 104–116
6. Mongrand, S., Morel, J., Laroche, J., Claverol, S., Carde, J. P., Hartmann, M. A., Bonneu, M., Simon-Plas, F., Lessire, R., and Bessoule, J. J. (2004)

J. Biol. Chem. **279,** 36277–36286
7. Coursol, S., Le Stunff, H., Lynch, D. V., Gilroy, S., Assmann, S. M., and Spiegel, S. (2005) *Plant Physiol.* **137,** 724–737
8. Ng, C. K. Y., Carr, K., McAinsh, M. R., Powell, B., and Hetherington, A. M. (2001) *Nature* **410,** 596–599
9. Liang, H., Yao, N., Song, J. T., Luo, S., Lu, H., and Greenberg, J. T. (2003) *Genes Dev.* **17,** 2636–2641
10. Wang, H., Li, J., Bostock, R. M., and Gilchrist, D. G. (1996) *Plant Cell* **8,** 375–391
11. Maceyka, M., Milstien, S., and Spiegel, S. (2005) *Prostaglandins Other Lipid Mediat.* **77,** 15–22
12. Cuvillier, O., Pirianov, G., Kleuser, B., Vanek, P. G., Coso, O. A., Gutkind, S., and Spiegel, S. (1996) *Nature* **381,** 800–803
13. Merrill, A. H., Jr., Sullards, M. C., Allegood, J. C., Kelly, S., and Wang, E. (2005) *Methods* **36,** 207–224
14. Iro, S., Ohnishi, M., and Fujino, Y. (1985) *Agric. Biol. Chem.* **49,** 539–540
15. Ohnishi, M., Ito, S., and Fujino, Y. (1983) *Biochim. Biophys. Acta.* **752,** 416–422
16. Ohnishi, M., and Fujino, Y. (1982) *Lipids* **17,** 803–809
17. Sastry, P. S., and Kates, M. (1964) *Biochemistry* **3,** 1271–1280
18. Cahoon, E. B., and Lynch, D. V. (1991) *Plant Physiol.* **95,** 58–68
19. Imai, H., Morimoto, Y., and Tamura, K. (2000) *J. Plant Physiol.* **157,** 453–456
20. Carter, H. E., Gigg, R. H., Law, J. H., Nakayama, T., and Weber, E. (1958) *J. Biol. Chem.* **233,** 1309–1314
21. Kaul, K., and Lester, R. L. (1975) *Plant Physiol.* **55,** 120–129
22. Carter, H. E., Strobach, D. R., and Hawthorne, J. N. (1969) *Biochemistry* **8,** 383–388
23. Kaul, K., and Lester, R. L. (1978) *Biochemistry* **17,** 3569–3575
24. Bonaventure, G., Salas, J. J., Pollard, M. R., and Ohlrogge, J. B. (2003) *Plant Cell* **15,** 1020–1033
25. Morrison, W. R., and Hay, J. D. (1970) *Biochim. Biophys. Acta.* **202,** 460–467
26. Merrill, A. H., Jr., Caligan, T. B., Wang, E., Peters, K., and Ou, J. (2000) *Methods Enzymol.* **312,** 3–9
27. Bligh, E. G., and Dyer, W. J. (1959) *Can. J. Biochem. Physiol.* **37,** 911–917
28. Nichols, B. W. (1963) *Biochim. Biophys. Acta.* **70,** 417–422
29. Christie, W. W. (2003) *Lipid Analysis*, 3rd Ed., The Oily Press, Bridgewater, UK
30. Hanson, B. A., and Lester, R. L. (1980) *J. Lipid Res.* **21,** 309–315
31. Toledo, M. S., Suzuki, E., Straus, A. H., and Takahashi, H. K. (1995) *J. Med. Vet. Mycol.* **33,** 247–251
32. Lester, R. L., and Dickson, R. C. (2001) *Anal. Biochem.* **298,** 283–292
33. Wells, G. B., Dickson, R. C., and Lester, R. L. (1996) *J. Bacteriol.* **178,** 6223–6226
34. Spassieva, S. D., Markham, J. E., and Hille, J. (2002) *Plant J.* **32,** 561–572
35. Levery, S. B., Toledo, M. S., Straus, A. H., and Takahashi, H. K. (2001) *Rapid Commun. Mass Spectrom.* **15,** 2240–2258
36. Costello, C. E., and Vath, J. E. (1990) *Methods Enzymol.* **193,** 738–768
37. Singh, B. N., Costello, C. E., and Beach, D. H. (1991) *Arch. Biochem. Biophys.* **286,** 409–418